Journal of Power Sources 253 (2014) 300–304

Contents lists available at ScienceDirect

Journal of Power Sources

journal homepage: www.elsevier.com/locate/jpowsour

Short communication

High-performance polyaniline counter electrode electropolymerized in presence of sodium dodecyl sulfate for dye-sensitized solar cells

Yin Qiu [a,b], Shan Lu [b], Shasha Wang [a,b], Xuehua Zhang [b,*], Shengtai He [a,*], Tao He [b,*]

[a] School of Materials Science and Engineering, Tianjin Polytechnic University, Tianjin 300387, China
[b] National Center for Nanoscience and Technology, Beijing 100190, China

HIGHLIGHTS

- SDS can act as both dopant and surfactant during PANI electropolymerization.
- SDS can improve the microstructure and conductivity of resultant PANI films.
- PANI films prepared with SDS have high catalytic activity on I_3^- reduction.
- PANI-SDS CE based DSSCs exhibit comparable power conversion efficiency to Pt CE.

GRAPHICAL ABSTRACT

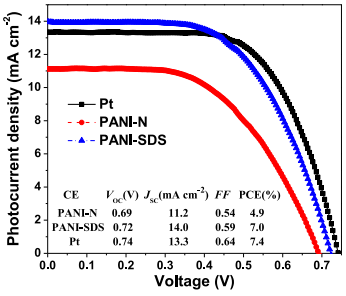

ARTICLE INFO

Article history:
Received 23 August 2013
Received in revised form
4 November 2013
Accepted 12 December 2013
Available online 19 December 2013

Keywords:
Polyaniline
Sodium dodecyl sulfate
Electropolymerization
Electrocatalytic activity
Counter electrodes
Dye-sensitized solar cells

ABSTRACT

Polyaniline (PANI) counter electrode (CE) has been fabricated for dye-sensitized solar cells (DSSCs) via electropolymerization in the presence of sodium dodecyl sulfate (SDS), which can act as both dopant and surfactant. The introduction of SDS in the synthetic solution for PANI can improve the microstructure and conductivity of resultant thin film and greatly increase the catalytic activity of the as-prepared PANI film for I_3^- reduction. The DSSCs based on the resultant PANI CEs achieve a remarkable power conversion efficiency of 7.0%, about 95% of that based on conventional Pt CEs (7.4%). The results indicate that the PANI film prepared with SDS may substitute the expensive Pt as the CEs for DSSCs application.

1. Introduction

As a typical photoelectrochemical cell, dye-sensitized solar cells (DSSCs) have been widely studied by virtue of relatively high energy conversion efficiency, low-cost, easy fabrication and friendly to environmental [1]. The role of counter electrode (CE) in DSSCs is to collect electrons flowing from external circuit, as well as to catalyze the regeneration of redox mediator. Thus, a good CE should have high conductivity, high electrocatalytic activity for I^-/I_3^- redox reaction, good chemical stability, and low cost. Although Pt has been used as the most popular CEs for DSSCs, its high cost, abundance deficiency, and easy corrosion in triiodide solution make it unsuitable for cost-effective fabrication and long-term stability of DSSC [2,3]. Thus, Pt-free materials with low cost and good stability have been explored as catalysts for DSSCs, mainly based on carbon materials [4–6], transition metal oxides and sulphides [7–12], and organic conducting polymers [13–21].

* Corresponding authors. Tel.: +86 10 8254 5655; fax: +86 10 6265 6765.
E-mail addresses: zhangxh@nanoctr.cn (X. Zhang), sht-he@tjpu.edu.cn (S. He), het@nanoctr.cn (T. He).

0378-7753/$ – see front matter © 2013 Elsevier B.V. All rights reserved.
http://dx.doi.org/10.1016/j.jpowsour.2013.12.061

Polyaniline (PANI) has been studied as a promising candidate to substitute Pt for DSSCs due to its high conductivity, good environmental stability, low cost, facile synthesis, and high catalytic activity for I_3^- reduction [17–21]. Compared with that prepared by chemical oxidation, PANI film synthesized via electropolymerization has merits of higher purity, better adhesivity, in-situ fabrication at low temperature, and the like, which exhibits great potential application in large-scale plastic solar cells. The presence of a surfactant in synthetic solution can significantly modify the properties of the obtained polymers [22]. For example, sodium dodecyl sulfate (SDS) has been used extensively as the surfactant/dopant for micelle/emulsion polymerization because SDS can form micelles in aqueous solution by the aid of the hydrophobic alkyl chain and the hydrophilic anionic charge. The morphology, conjugation, doping degree, and conductivity of the resultant polymer film can thus been tuned [23].

The morphology and conductivity of the CEs have a great impact on the DSSC performance; while so far no work is reported about the PANI CEs prepared using SDS as the surfactant/dopant for DSSCs application. Herein, we fabricated PANI films via in-situ electropolymerization in the presence of SDS (PANI-SDS) and used them as the CEs in DSSCs. The PANI films were synthesized under a constant bias (0.8 V vs. SCE) using a same charge capacity (0.8 C) for all of the samples. The performance of the DSSCs based on PANI-SDS CE has been compared with those based on both the control (Pt CE) and that prepared without SDS (PANI-N). The morphology, doping degree, electric conductivity, and the electrocatalytic activity of the PANI films have also been discussed in detail.

2. Experimental

2.1. Preparation of the PANI CEs

The PANI films were prepared by electrochemical polymerization on FTO glass (fluorine-doped tin oxide, 14 Ω □$^{-1}$, Wuhan Ge'ao Co., Ltd., China) with a CHI 660D potentiostat (CH Instrument, China). Before polymerization, the FTO substrates were pretreated using an ultrasonic bath in detergent, acetone, deionized water, and 2-propanol for 15 min, respectively. The polymerization was performed under a constant bias of 0.8 V at a same charge of 0.8 C for all of the samples at room temperature. A Pt plate was used as the counter electrode and a saturated calomel electrode (SCE) served as the reference electrode. The electropolymerization solution was composed of 0.25 M aniline, 0.20 M H_2SO_4, with (PANI-SDS) or without (PANI-N) 0.15 M SDS in water. The obtained PANI films were then washed copiously with water and dried at 70 °C for 1 h in air for use. For comparison, Pt CEs were prepared by thermal decomposition of H_2PtCl_6 (30 mM in isopropanol) on FTO substrates at 385 °C for 30 min.

2.2. Fabrication of DSSCs devices

The TiO_2 (20 nm, Wuhan Ge'ao Co., Ltd., China) films were fabricated on FTO by using doctor-blade technique, followed by sintering at 125, 325, 375, 450, and 500 °C for 6, 15, 10, 15, and 10 min, respectively. The thickness of the obtained TiO_2 photoanodes was about 8 μm and the active area was 0.35 cm^2. Then they were treated with 0.02 M $TiCl_4$ solution at 70 °C for 30 min, followed by being sintered at 450 °C for 30 min again. After cooling down to 80 °C, they were immersed for 12 h into a mixture solution of acetonitrile and t-butanol (volume ratio of 1:1) containing 0.5 mM N719 dye (Solaronix). The sandwich-type solar cells consisted of a dye-sensitized TiO_2 film as working electrode, the as-prepared PANI or Pt electrode as CE, and an electrolyte solution containing 0.1 M LiI, 0.05 M I_2, 0.6 M 1,2-dimethyl-3-propylimidazolium iodide, and 0.5 M 4-tert-butylpyridine in 3-methoxyacetonitrile.

2.3. Characterization and measurements

The morphology was characterized by the field-emission scanning electron microscopy (FE-SEM Hitachi S-4800). Absorption spectra were collected using a Lambda 750 UV/Vis/NIR spectrophotometer. The X-ray photoelectron spectroscopy (XPS) spectra were obtained by a Thermo Scientific ESCALAB 250 instrument. Electrochemical catalytic activity was evaluated by cyclic voltammetry (CV) measurements using a three-electrode system in an acetonitrile solution containing 10 mM LiI, 1.0 mM I_2, and 0.1 M $LiClO_4$ with the CHI 660D electrochemical workstation. The scan rate is 50 mV s^{-1}. A Pt plate and an SCE were used as counter and reference electrode, respectively. The measurements of double layer capacitance were performed on the CHI 660D. Electrochemical impedance spectra (EIS) of the DSSCs were measured in the dark under a DC bias of −0.7 V with a frequency range of 0.01–10^5 Hz using the CHI 660D electrochemical workstation. Photovoltaic performance of the DSSCs were measured using a solar simulator (Model 69907, Oriel) and Keithley source meter (2420) under illumination of AM 1.5G light (85 mW cm^{-2}), a mask with a window of 0.15 cm^2 was clipped on the TiO_2 side to define the active area of the cells.

3. Results and discussion

3.1. Photovoltaic performance of the DSSCs

Fig. 1 shows the current density–voltage (J–V) characteristics of the DSSCs based on the CEs of PANI-SDS, PANI-N and Pt. The derived photovoltaic parameters are listed in the inset of Fig. 1. The DSSC based-on PANI-SDS CE shows a power conversion efficiency (PCE) of 7.0%, with an open-circuit voltage (V_{oc}) of 0.72 V, short-circuit current density (J_{sc}) of 14.0 mA cm^{-2}, and fill factor (FF) of 0.59. Such a PCE is much higher than that based on PANI-N CE (4.9%) and is about 95% of that using Pt CE (7.4%), indicting a high electrocatalytic activity of PANI CEs prepared with SDS on I_3^- reduction.

3.2. Surface morphology of the PANI films

The morphology of as-prepared PANI films was studied using SEM images. Both the films prepared with and without SDS have a strongly bounded, compact graniform thin layer of PANI on the surface of FTO substrate (Fig. 2). For PANI-N, some cauliflower-

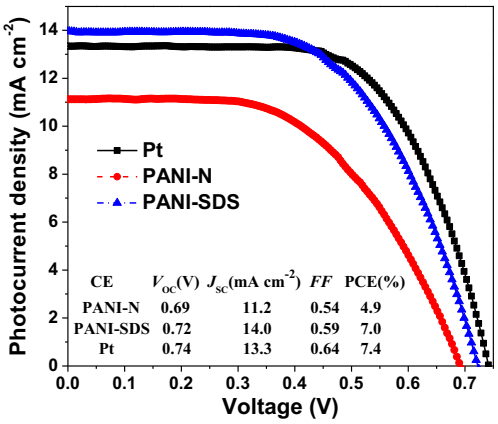

Fig. 1. J–V curves of the DSSCs based on PANI and Pt CEs.

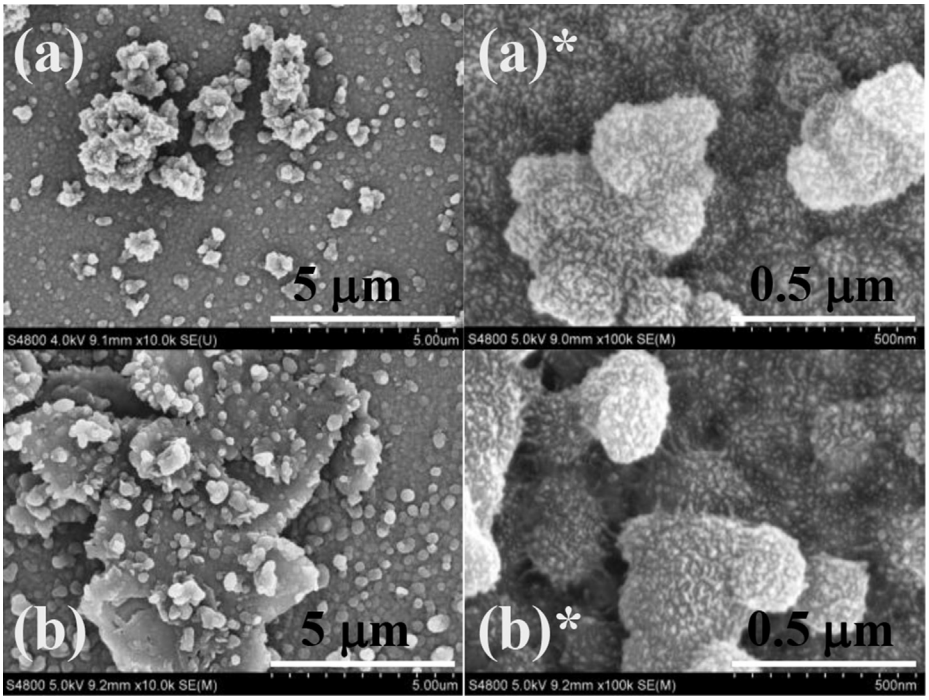

Fig. 2. SEM images of (a) PANI-N and (b) PANI-SDS films. The (a)* and (b)* are the zoom-in images of (a) and (b), respectively.

shaped PANI distributes randomly on the first layer. The high magnification image indicates that both the grains and flowers are composed of small fluffy granules with a diameter of about 15 nm (Fig. 2(a)*), which may be formed by the twisted and coiled PANI chains. While for PANI-SDS, some big block-like PANI is present on the first compact layer, which is composed of porous microvillus structure (Fig. 2(b)*). Since SDS molecules can act as both dopant and surfactant during electropolymerization, this may be ascribed to the large size of dodecyl sulfate anion (DS^-) and high local concentration of aniline monomer in the micellar reaction medium. The resultant porous structure of PANI-SDS film can facilitate the penetration of electrolyte in CEs of DSSCs. A reduced charge transfer resistance at the CE/electrolyte interface is thus expected.

3.3. Structure and conductivity characterization of the PANI films

The structure and conductivity of the as-prepared films were first studied by the absorption spectra. The PANI films obtained with and without SDS exhibit a similar curve shape, with two major absorption peaks (Fig. 3). The peak at around 335 nm (λ_1) originates from the $\pi-\pi^*$ transition centered in the benzenoid rings, and the one in the NIR region (λ_2) corresponds to the charged cationic species (polaron band transition), indicating that the obtained PANI films are both in doping states [24]. The intensity (A) of the absorption peaks for both PANI films hardly changes because they are electropolymerized at the same charge capacity. However, λ_2 of PANI-SDS (762 nm) exhibits a considerable red shift compared with that of PANI-N (704 nm), suggesting a longer conjugation length of the PANI-SDS backbone. This is because the surfactant ions (DS^-) can produce some template effects at electrode/solution interface, improving the organization of PANI chains. Furthermore, the DS^- can be incorporated into the polymer acting as dopants during electropolymerization. The hydrophobic alkyl chain of DS^- can decrease the molecular interaction of the PANI chains, facilitating the formation of much more ordered PANI chains.

The doping degree of the PANI films was calculated from XPS analysis. The binding energies at about 399.6 eV and 168.6 eV are attributed to the N_{1s} in PANI backbone and S_{2p} in SO_4^{2-} (and/or DS^-), respectively [25]. The percentage of N and S elements for each sample can be calculated according to the XPS spectra (Table 1). The doping degree of PANI is thus estimated from the atomic ratio of S to N (S/N). The value of S/N of PANI-SDS (0.40) is much higher than that of PANI-N (0.25), indicating a much higher doping degree of the counter anion for PANI-SDS (about one dopant counter anion per 2.5 aniline) than PANI-N (about one dopant counter anion per 4 aniline). The S_{2p} spectra of PANI-N consist of two peaks centered at 168.3 eV and 169.5 eV upon deconvolution (Fig. 4), corresponding to the respective spin orbit of $S_{2p1/2}$ and $S_{2p3/2}$ doublet peak in SO_4^{2-}. Besides this S_{2p} XPS signal, it is noted that a new pair of peak appear in the S_{2p} spectra for PANI-SDS (Fig. 4, 168.9 eV and 170.1 eV), indicating the presence of DS^-. So the DS^- ions are doped in PANI. The doping degree of SO_4^{2-} and DS^- in PANI-SDS is around 0.256 and 0.145, respectively. Thus, the increased doping degree of PANI-SDS is ascribed to the DS^- dopant. It is known that the electric conductivity of a polymer is closely related to its doping degree,

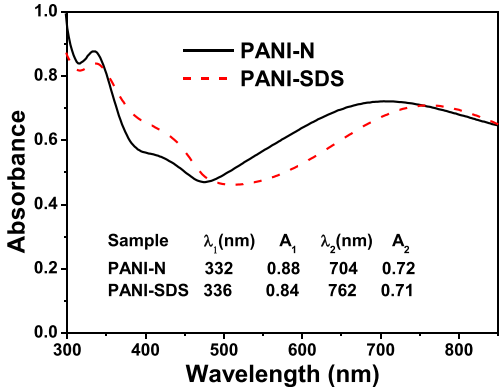

Fig. 3. Absorption spectra of the PANI films, inset shows the maximum absorption peaks (λ) and the corresponding absorbance (A).

Table 1
Atomic percentage of N and S elements in the as-prepared PANI films derived from XPS results.

Sample	C (%)	N (%)	S (%)	S/N
PANI-N	76.91	10.97	2.74	0.25
PANI-SDS	77.76	7.93	2.04 (SO_4^{2-}) + 1.15 (DS^-)	0.40

conjugation length, and ordering of the backbone. Therefore, PANI-SDS is expected to exhibit a higher conductivity than PANI-N.

3.4. EIS characteristics of DSSCs

EIS analysis was carried out using the DSSCs to study charge transfer resistance at the interface (Fig. 5). The impedance parameters are derived in terms of the equivalent circuit shown in Fig. 5 (Table 2). The R_{ct} is the charge transfer impedance at electrode/electrolyte interface (including both interfaces of working electrode/electrolyte and CE/electrolyte), W represents Warburg diffusion impedance, Cdl is double-layer capacitance, and R_s is impedance contributed from the contact resistance, bulk electrolyte and electrodes. Since all of the components in the DSSCs are the same except the CEs, the change in the R_{ct} can be attributed mainly to the difference in CEs, although the measured values include the charge transfer impedance at all of the interfaces. Thus, a lower R_{ct} corresponds to a higher electron transfer rate between the CE and electrolyte, i.e. a higher catalytic activity on the reduction of I_3^- to I^-. It is found that the DSSC based on PANI-SDS CE shows a similar R_{ct} value (150.5 Ω) to that on Pt CE (147.9 Ω), which is lower than that on PANI-N CE (239.1 Ω). This is because the PANI film prepared with the addition of SDS has a higher conductivity as well as a more porous microstructure than that without SDS.

3.5. Electrocatalytic activity of PANI films for I^-/I_3^-

CV was used to evaluate the electrocatalytic activity of the as-prepared PANI films on I_3^- reduction. The CV curves of I^-/I_3^- redox reaction with PANI-N, PANI-SDS, and Pt electrodes exhibits a similar behavior (Fig. 6), with two pairs of redox peaks in the scanning range of −0.5 to 1.3 V (vs. SCE). The left one is assigned to $3I^- \leftrightarrow I_3^- + 2e^-$, and the right one corresponds to $2I_3^- \leftrightarrow 3I_2 + 2e^-$ [26]. It can be seen that PANI-SDS shows a higher current density for I_3^- reduction than Pt and PANI-N, indicating that PANI-SDS has a higher catalytic activity on the I_3^- reduction to I^- than PANI-N. In

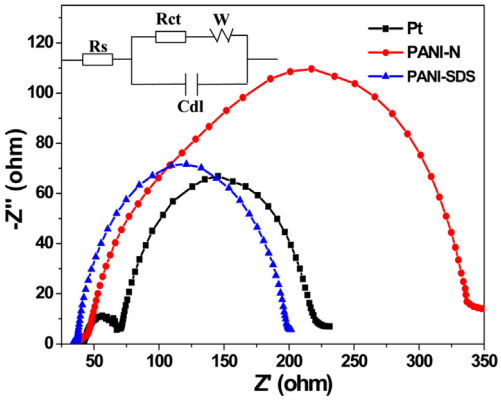

Fig. 5. Nyquist plots of the DSSCs based on PANI and Pt CEs, inset shows the equivalent circuit employed to simulate the spectra.

Table 2
EIS parameters of the DSSCs derived from the spectra shown in Fig. 5.

CE	R_s (Ω)	R_{ct} (Ω)	PCE (%)
PANI-N	43.7	239.1	4.9
PANI-SDS	36.5	150.5	7.0
Pt	52.2	147.9	7.4

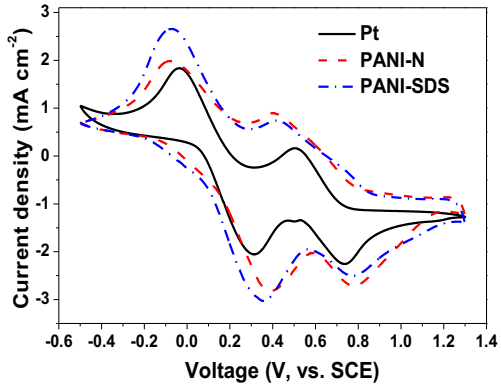

Fig. 6. CV curves of the I^-/I_3^- redox couple on PANI and Pt electrodes.

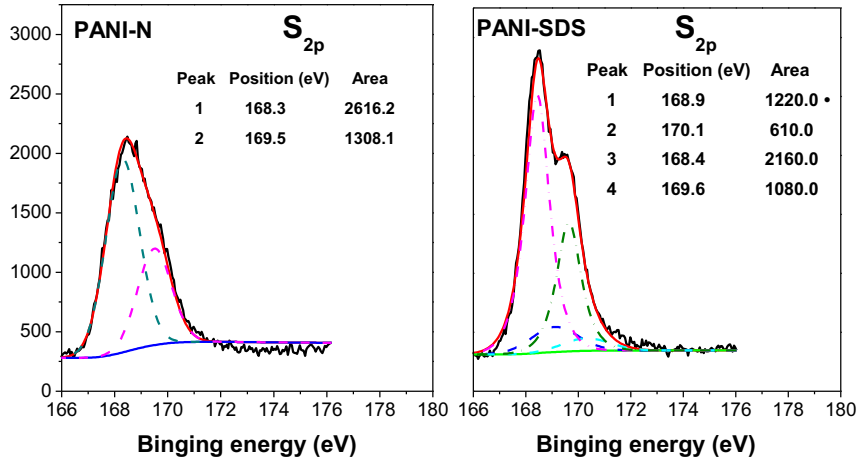

Fig. 4. S_{2p} XPS spectra of PANI-N and PANI-SDS films.

addition, the effective electrochemical active area (EEAA) is estimated using double-layer capacitance (C_d) measurements. A larger C_d means a higher EEAA. The value of C_d for PANI-N and PANI-SDS is 18.24 and 18.87 μF, respectively. Thus, PANI-SDS has a similar EEAA to PANI-N. This is reasonable since the same charge was used for the electro-polymerization. Hence, the superior catalytic activity of PANI-SDS is mainly caused by its high conductivity and low charge transfer resistance, as well as the porous microstructure.

4. Conclusions

In summary, the SDS introduced into the solution for PANI synthesis can act as both surfactant and dopant, leading to controllable modulation of the doping degree, conjugation length, and micro-structure of the as-prepared PANI films. Accordingly, the electric conductivity, interface charge transfer rate, catalytic activity on I_3^- reduction, and porosity of the obtained PANI films can be improved, resulting in an enhanced device efficiency. The DSSC based on PANI-SDS CE exhibits a PCE of 7.0%, up to 95% of that with Pt CE (7.4%) under the same conditions. The results indicate that the PANI film prepared with SDS may substitute the expensive Pt as the CEs for DSSC application, especially for the large-scale flexible devices.

Acknowledgments

This work was supported by the National Natural Science Foundation of China (21203039), Ministry of Science and Technology of China (2010DFB63530), Hundred-Talent Program of Chinese Academy of Sciences, and Tianjin Research Program of Applied Basic & Cutting-Edge Technologies (09JCYBJC27200).

References

[1] B. O'Regan, M. Grätzel, Nature 353 (1991) 737–740.
[2] N. Papageorgiou, W.F. Maier, M. Grätzel, J. Electrochem. Soc. 144 (1997) 876–884.
[3] E. Olsen, G. Hagen, S.E. Lindquist, Sol. Energy Mater. Sol. Cells 63 (2000) 267–273.
[4] H. Wang, Y.H. Hu, Energy Environ. Sci. 5 (2012) 8182–8188.
[5] F. Hao, P. Dong, J. Zhang, Y.C. Zhang, P.E. Loya, R.H. Hauge, J.B. Li, J. Lou, H. Lin, Sci. Rep. 2 (2012) 368–373.
[6] L.H. Chang, C.K. Hsieh, M.C. Hsiao, J.C. Chiang, P.I. Liu, K.K. Ho, C.M. Ma, M.Y. Yen, M.C. Tsai, C.H. Tsai, J. Power Sources 222 (2013) 518–525.
[7] M.K. Wang, A.M. Anghel, B. Marsan, N.C. Ha, N. Pootrakulchote, S.M. Zakeeruddin, M. Grätzel, J. Am. Chem. Soc. 131 (2009) 15976–15977.
[8] F. Gong, H. Wang, X. Xu, G. Zhou, Z.S. Wang, J. Am. Chem. Soc. 134 (2012) 10953–10958.
[9] F. Gong, X. Xu, Z.Q. Li, G. Zhou, Z.S. Wang, Chem. Commun. 49 (2013) 1437–1439.
[10] X. Chen, Y. Hou, B. Zhang, X.H. Yang, H.G. Yang, Chem. Commun. 49 (2013) 5793–5795.
[11] Y. Hou, D. Wang, X.H. Yang, W.Q. Fang, B. Zhang, H.F. Wang, G.Z. Lu, P. Hu, H.J. Zhao, H.G. Yang, Nat. Commun. 4 (2013) 1583–1590.
[12] W. Zhao, X.L. Zhu, H. Bi, H.L. Cui, S.R. Sun, F.Q. Huang, J. Power Sources 242 (2013) 28–32.
[13] H.N. Tian, Z. Yu, A. Hagfeldt, L. Kloo, L.C. Sun, J. Am. Chem. Soc. 113 (2011) 9413–9422.
[14] K.M. Lee, P.Y. Chen, C.Y. Hsu, J.H. Huang, W.J. Ho, H.C. Chen, K.C. Ho, J. Power Sources 188 (2009) 313–318.
[15] X.H. Zhang, S.S. Wang, S. Lu, J. Su, T. He, J. Power Sources, power-D-13-01944.
[16] J.B. Xia, L. Chen, S. Yanagida, J. Mater. Chem. 21 (2011) 4644–4649.
[17] H. Wang, Q.Y. Feng, F. Gong, Y. Li, G. Zhou, Z.S. Wang, J. Mater. Chem. A 1 (2013) 97–104.
[18] Z.P. Li, B.X. Ye, X.D. Hu, X.Y. Ma, X.P. Zhang, Y.Q. Deng, Electrochem. Commun. 11 (2009) 1768–1771.
[19] Q.H. Li, J.H. Wu, Q.W. Tang, Z. Lan, P.J. Li, J.M. Lin, L.Q. Fan, Electrochem. Commun. 10 (2008) 1299–1302.
[20] S.S. Wang, S. Lu, X.M. Li, X.H. Zhang, S.T. He, T. He, J. Power Sources 242 (2013) 438–446.
[21] Q.D. Tai, B. Chen, F. Guo, S. Xu, H. Hu, B. Sebo, X.Z. Zhao, ACS Nano 5 (2011) 3795–3799.
[22] D.C. Wu, F. Xu, B. Sun, R.W. Fu, H.K. He, K. Matyjaszewski, Chem. Rev. 112 (2012) 3959–4015.
[23] N. Kuromoto, A.M. Genies, Syn. Met. 68 (1995) 191–194.
[24] S. Shreepathi, R. Holze, Chem. Mater. 17 (2005) 4078–4085.
[25] C.D. Wagner, W.M. Riggs, L.E. Davis, J.F. Moulder, G.E. Muilenberg, Handbook of X-ray Photoelectron Spectroscopy, Perkin-Elmer Corp., Eden Prairie, Minneapolis, 1979.
[26] V.A. Macagno, M.C. Giordano, Electrochim. Acta 14 (1969) 335–357.